The Elastic Properties of the *Cryptococcus neoformans* Capsule

Susana Frases,[†*] Bruno Pontes,[‡] Leonardo Nimrichter,[§] Marcio L. Rodrigues,[§] Nathan B. Viana,[‡¶] and Arturo Casadevall[†‖]

[†]Department of Microbiology and Immunology, Albert Einstein College of Medicine, The Bronx, New York; [‡]LPO-COPEA, Instituto de Ciências Biomédicas, Universidade Federal do Rio de Janeiro, Rio de Janeiro, Brazil; [§]Laboratório de Estudos Integrados em Bioquímica Microbiana, Instituto de Microbiologia Professor Paulo de Góes, Universidade Federal do Rio de Janeiro, Rio de Janeiro, Brazil; [¶]Division of Infectious Diseases of the Department of Medicine, Albert Einstein College of Medicine, The Bronx, New York; and [‖]Instituto de Física, Universidade Federal do Rio de Janeiro, Rio de Janeiro, Brazil

ABSTRACT Microbial capsules are important for virulence, but their architecture and physical properties are poorly understood. The human pathogenic fungus *Cryptococcus neoformans* has a large polysaccharide capsule that is necessary for virulence and is the target of protective antibody responses. To study the *C. neoformans* capsule we developed what we believe is a new approach whereby we probed the capsular elastic properties by applying forces using polystyrene beads manipulated with optical tweezers. This method allowed us to determine the Young's modulus for the capsule in various conditions that affect capsule growth. The results indicate that the Young's modulus of the capsule decreases with its size and increases with the Ca^{2+} concentration in solution. Also, capsular polysaccharide manifests an unexpected affinity for polystyrene beads, a property that may function in attachment to host cells and environmental structures. Bead probing with optical tweezers provides a new, nondestructive method that may have wide applicability for studying the effects of growth conditions, immune components, and drugs on capsular properties.

INTRODUCTION

Polysaccharide (PS) capsules are common in bacterial pathogens, but in fungi they are exclusive to *Cryptococcus* genus (1). *Cryptococcus neoformans* is an encapsulated fungal pathogen that is acquired by human and animal hosts through inhalation of environmental infectious propagules (2). *C. neoformans* is a round or oval-shaped yeast cell. The size of the organism is ~2.5 μm without the capsular PS. The capsule is found immediately outside the cell wall and can vary in size from 1 to 50 μm, depending on the cell type, environment, and growth conditions. Capsule architecture is characterized by a complex PS network connected to the cell wall and extending to variable distances into the extracellular space (2).

In *C. neoformans*, the components of the capsular network constitute the main fungal virulence factor (2). Capsular components include two different types of PS, galactoxylomannan and glucuronoxylomannan (GXM). Galactoxylomannan, a low-molecular-weight α1–6-linked galactan containing different types of mannosyl and xylosyl substitutions, is the minor component (3,4). GXM is a high-molecular-weight PS that accounts for ~90% of the mass of capsular and shed PS (4,5). GXM is an α1–3-linked mannan containing β1,2 and β1,4 xylosyl substitutions, as well as β1,2-linked glucuronyl residues (1). This molecule, which is also *O*-acetylated at the carbon 6 of some of the mannosyl units, forms a heterogeneous macromolecular complex with a molecular mass in the range 1–7 $\times$ 10^7 Da (4).

Little is known about the molecular architecture of microbial capsules and the mechanisms by which these complexes enlarge. In *C. neoformans*, capsule enlargement has been associated with virulence (6) and protection of the fungus against host defense mechanisms such as phagocytosis and oxidative burst (7–9). In fact, capsule size in *C. neoformans* is regulated by several environmental conditions, including CO_2 availability, iron concentration, and medium osmolarity (7–11). Different host elements apparently regulate the capsular architecture of *C. neoformans*, since capsule thickness varies during cryptococcosis depending on which tissue is infected (12).

Capsule enlargement in cryptococci occurs by apical growth (6) and there is evidence that capsule size is regulated at the level of individual PS molecules (13). Consistent with this notion, capsule growth has been shown to result from enlargement of PS molecules (14). Given that its assembly involves noncovalent attachment of PS fibrils both to the cell wall (15) and to each other, it is likely that many aspects of capsule construction are directly related to the physical-chemical properties of the PS molecules. For example, there is evidence that capsular assembly is at least partly the result of inherent PS properties that promote self-aggregation (16). In fact, a number of techniques have shown that *C. neoformans* PS aggregation depends on the interaction of anionic PSs with divalent cations (16). Pure GXM is highly viscous and its ability to self-aggregate directly affects its physical and biological properties, as well as impacting capsule assembly (16,17). Since physical properties of the capsular PS may largely determine capsule architecture and the

Submitted January 26, 2009, and accepted for publication April 15, 2009.

Susana Frases and Bruno Pontes contributed equally to this work.

Nathan B. Viana and Arturo Casadevall share senior authorship.

*Correspondence: scarvaja@aecom.yu.edu

Editor: Richard E. Waugh.

0006-3495/09/08/0937/9 $2.00

doi: 10.1016/j.bpj.2009.04.043

biological properties of capsular components, elastic properties of the *C. neoformans* capsular PS may be key to physiological and pathogenic events.

In bacteria, atomic force microscopy and optical traps have been used to characterize elastic properties of bacterial cell walls, to measure their stiffness and structural properties (18–20). In this study, we developed what we believe is a new approach to investigate the elastic properties of the *C. neoformans* capsule using its interaction with polystyrene beads and optical tweezers. In fact, the response of the PS capsule to stress should be more complicated than that of normal liquids or solids, since it is composed of molecules that can be studied by viscoelasticity models (21). Due to the high viscosity of pure PS solutions, we considered the capsule as an elastic solid material. We measured the elastic modulus, also known as Young's modulus, for *C. neoformans* yeast cells in different conditions known to affect the architecture of the capsule. The results indicate that the elastic properties of the *C. neoformans* capsule are dependent on the yeast cell capsule size, a finding that implies significant differences in PS structure, mechanical properties, and/or packing as the capsule enlarges.

MATERIALS AND METHODS

Optical tweezers setup

The optical tweezers (OT) system (22) was constructed using an infrared Nd:YAG laser with a wavelength of 1.064 μm (Quantronix, East Setauket, NY) that has a Gaussian intensity profile (TEM_{00} mode), and maximum power of 3 W. The laser beam intensity profile has a half-width of 2.3 $\pm$ 0.2 mm at the back focal plane of the objective lens as described in Viana et al. (23). The optical trap is constructed in an inverted Nikon Eclipse TE300 microscope (Nikon, Melville, NY), equipped with a PLAN APO 60X 1.4 NA DIC H Nikon objective used to create the optical trap.

Sample velocity calibration

To measure the sample velocity, we used a polystyrene bead with radius $a = 1.52 \pm 0.02$ μm (Polysciences, Warrington, PA) attached to the coverslip. The optical trap was turned off and then the stage was moved. The stage movement was controlled by a Prior (Prior Scientific, Rockland, MA) positioning system adapted to the microscope. Step motors actuate in the xy microscope-stage directions, moving the samples respectively. Bead displacement was recorded simultaneously with an FG-7 frame grabber (Scion Corporation, Torrance, CA). The images were analyzed using ImageJ (National Institutes of Health,Washington, D.C.) software to determine the bead's position. The sample velocity (V) was then determined by a linear fit of the bead position as a function of time.

Trap calibration

To calibrate the OT, the same polystyrene bead ($a = 1.52 \pm 0.02$ μm) was first captured and then the sample was set to move with velocity (V). Images of the entire process were recorded. The center-of-mass position of the trapped bead, ρ, was obtained by image analysis using the centroid-finding algorithm of the ImageJ software (National Institutes of Health). $\Delta\rho$ was defined as the difference between the bead center-of-mass position when the sample is moving with velocity V and when the sample is not moving:

$$\Delta\rho = \rho(V) - \rho(0). \quad (1)$$

For small displacements of the bead in the trap (~1 μm) we have

$$\Delta\rho = \frac{\beta}{\kappa_\perp} V, \quad (2)$$

where $\kappa_\perp$ is the trap stiffness in relation to the plane of the image (perpendicular to the beam direction of propagation) and β is the Stokes friction coefficient. β is given by the Stokes-Faxen law (23):

$$\beta = 6\pi\eta a\left[1 - \frac{9}{16}\left(\frac{a}{h}\right) + \frac{1}{8}\left(\frac{a}{h}\right)^3 - \frac{45}{256}\left(\frac{a}{h}\right)^4 - \frac{1}{16}\left(\frac{a}{h}\right)^5\right]^{-1}, \quad (3)$$

where a is the bead radius, η is the solution viscosity, and h is the distance of the center of mass of the bead to the glass coverslip of the sample. By moving the sample with different values of V and measuring the respective center-of-mass displacement of the bead, the trap stiffness $\kappa_\perp$ is obtained.

Using the trap calibration, a displacement of a trapped bead in relation to its trap equilibrium position multiplied by the value of the trap stiffness gives the force on the sphere:

$$F = \kappa_\perp \Delta\rho. \quad (4)$$

The trap stiffness value can be increased or decreased by changing the laser beam power (24). Trap calibration measurements were performed for each value of power used.

C. neoformans culture

C. neoformans strain H99 yeast cells were grown in a minimal medium composed of glucose (15 mM), $MgSO_4$ (10 mM), KH_2PO_4 (29.4 mM), glycine (13 mM), and thiamine-HCl (3 μM), pH 5.5 with shaking (150 rpm) at 30°C. Culture time varied according to the experiment being performed. Minimal medium is a chemically defined medium that induces capsule growth over time (14).

Measurement of the bead adhesion contact angle

Yeast cells (10^6 cells/ml) were washed in phosphate-buffered saline (PBS) and blocked with PBS containing 1% bovine serum albumin for 1 h at 37°C. Then, cells were incubated with 2 μg/mL of anticapsular monoclonal antibody (mAb) 18B7 (mouse IgG1 (25)) for 1 h at 37°C. After washing the excess of antibody with PBS, 10 μg/mL of fluorescein (FITC)-conjugated antibody to mouse-IgG-FITC was added and incubated for 1 h at 37°C. Cells were washed with PBS and added to a glass-bottom dish previously coated, overnight at 4°C, with 18B7 mAb. After 1 h of incubation at room temperature, and three washes with PBS, uncoated polystyrene beads were added to the cell plate. The plate was placed in the microscope and the optical trap was used to grab the beads in solution and place them in contact with the cell capsule. Images were taken in an inverted microscope (Eclipse TE300, Nikon) equipped with Plan APO 100× 1.4 NA DIC H. Fluorescence images were taken by a Cool Snap Pro Color Roper Scientific CCD camera (Media Cybernetics, Silver Spring, MD) that digitized them directly to the computer, and were captured employing ImagePro Plus (Media Cybernetics). Image analysis was performed with ImageJ and data analysis with Kaleidagraph (Synergy Software, Essex Junction, VT).

Young's modulus measurement

Glass-bottom dishes were coated with 10 μg/mL of mAb 18B7, as described above, and 200-μL suspensions of 10^4 *C. neoformans* cells in PBS were added to the plates and then incubated for 1 h at room temperature. After washing with PBS to remove nonadherent cells, polystyrene beads were added to the plate and the samples were placed in the OT system. To measure the Young's modulus of the PS capsule of *C. neoformans*, a polystyrene bead ($a = 1.52 \pm 0.02$ μm) was first captured with the OT and then

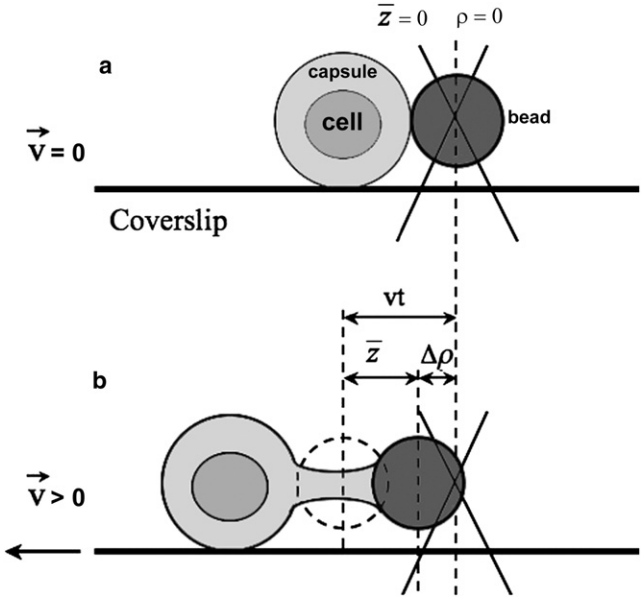

FIGURE 1 Proposed model for determination of the elastic properties of the *C. neoformans* capsule. (*a*) Initial situation where the bead (*solid bead*) is in its equilibrium position in the trap, $\rho = 0$, and the capsule is not deformed, $\bar{z} = 0$. (*b*) As the microscope stage moves left under controlled velocity, the cell adhered to the coverslip similarly moves to the left. There appears a ''tug of war'' between the cell and the optical tweezers. As a result, the trapped bead changes its equilibrium position, from $\rho(0)$ to $\rho(V)$, resulting in $\Delta\rho > 0$, and the capsule deforms, $\bar{z} > 0$, to balance the optical force.

pressed against the capsule for 1 min, to attach the bead to the fungus capsule. The microscope stage was then moved with a controlled velocity ($V = 0.071 \pm 0.002$ μm/s). As a result, the attached bead changed its equilibrium position in the trap and the fungal capsule deformed. Images of the entire process were captured using a CCD Hamamatsu C2400 camera (Hamamatsu, Japan) and, using ImageJ software, the change in equilibrium position of the trapped bead, $\Delta\rho$, was determined as a function of time. With this result the Young's modulus was determined.

A schematic representation of our experimental model is shown in Fig. 1. The force applied to the capsule is a function of time:

$$F(t) = \kappa_{\perp}\Delta\rho(t). \tag{5}$$

Following Laurent et al. (26), in the Supporting Material, we derive the relation between $F(t)$ and the deformation of the capsule, $\bar{z}(t)$:

$$F(t) = 2\pi aEg(\alpha)\bar{z}(t) \tag{6}$$

$$g(\alpha) = \frac{(1-\cos^3\alpha)}{2}\left(\frac{1-\cos\,\alpha}{1-\frac{1}{4}\cos^3\alpha-\frac{3}{4}\cos\,\alpha}\right), \tag{7}$$

a is the bead's radius, E is the capsule's Young's modulus, and α is the contact angle between the bead and the cell capsule (Fig. 2).

The geometry proposed in Fig. 1 leads to the relation

$$\bar{z}(t) = vt - \Delta\rho(t). \tag{8}$$

Therefore, when we substitute Eq. 5 and Eq. 6 into Eq. 8, we get

$$\Delta\,\rho(t) = \frac{v}{1+\frac{\kappa_{\perp}}{2\,\pi\,aE\,g(\alpha)}}\,t. \tag{9}$$

Then, E can be determined by measuring the slope, A, of the plot $\Delta\rho \times t$:

$$\Delta\rho(t) = At, \tag{10}$$

and

$$E = \frac{\kappa_{\perp}}{2\pi ag(\alpha)}\left(\frac{A}{v-A}\right). \tag{11}$$

Using the least-squares method to fit the theoretical model to the experiments, the values for the elastic modulus of *C. neoformans* capsule were determined.

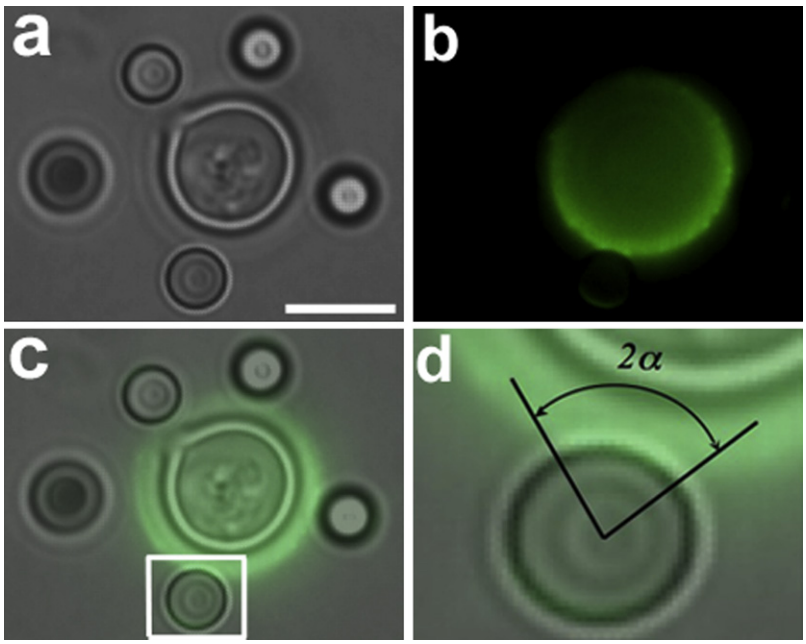

FIGURE 2 Measurement of the contact angle after attachment of beads to the capsule of *C. neoformans*. (*a*) Bright-field image showing four polystyrene beads attached to the *C. neoformans* capsule. (*b*) Corresponding immunofluorescence after capsule staining with 18B7 antibody. (*c*) Merging of the images shown in *a* and *b*. (*d*) A high-magnification look at the boxed zone in *c* showing the bead-capsule contact angle. Scale bar for *a–c*, 5μm.

Effect of divalent cations in elasticity of *C. neoformans* capsular cells

C. neoformans H99 cells were incubated overnight with 10 mM EDTA. EDTA was removed by three sequential washes with water; the cells were then suspended in $CaCl_2$ (0.2, 2, 6, 10, 15, or 20 mM) and incubated at room temperature for 2 h. Treated cells were placed into a glass-bottom dish previously coated with 10 μg/mL of mAb 18B7 and incubated for 1 h at room temperature. After washing for removal of unbound yeast cells, polystyrene beads were added to the plate. All measurements of Young's modulus were done as described before.

Young's modulus of *C. neoformans* Capsular polysaccharide as a function of capsule size and culture growth time

C. neoformans H99 cells were incubated in minimal media at 30°C for 7 days, as described above. The elastic properties were then determined according to the methodology described. Capsule size measurements were done by negative staining with India ink. The capsule sizes of 100 cells from 10 different fields for each culture time were measured using ImageJ software. Results were presented as mean $\pm$ SE for each condition. Capsular thickness was defined as the distance between the visualized cell wall and the edge of the capsule, represented by the exclusion of India ink.

Scanning electron microscopy

C. neoformans H99 cells were washed three times with PBS, transferred to 2.5% glutaraldehyde and incubated for 1 h at room temperature. The samples were serially dehydrated in alcohol, fixed in a critical-point drier model Samdri-790 (Tousimis Research Corporation, Rockville, MD), coated with gold-palladium model Desk-1 (Denton Vacuum, Moorestown, NJ), and viewed with a JEOL (Tokyo, Japan) JSM-6400 scanning electron microscope.

Effect of calcium on antibody binding by immunofluorescence

H99 *C. neoformans* cells were grown in minimal media, as described, for 3 days at 30°C. Cells were washed twice in PBS and incubated overnight with 10 mM of EDTA. EDTA was removed by three sequential washings with water. The cells were then suspended in $CaCl_2$ (0.2, 2, 6, 10, 15, or 20 mM) and incubated at room temperature for 2 h. Then, cells were washed again with water and blocked with PBS and 1% bovine serum albumin. After another serial washing, cells were incubated with 10 μg/mL of mAb 18B7 for 1 h at 37°C followed by addition of FITC-conjugated goat antibody to mouse IgG for detection of the primary antibody. The cell wall of *C. neoformans* cells was visualized by staining with UVITEX 2B (Polysciences). Cells were observed using an AX 70 microscope (Olympus, Melville, NY) equipped with fluorescence filters. Images were analyzed with ImageJ software. Measurements of 18B7 binding length and distance between the cell wall and the binding of 18B7 were performed for 50 cells of each group.

Adherence of polysaccharide to polystyrene plates as a function of Ca^{2+}

Capsular PS from H99 cells was extracted by dimethylsulfoxide (DMSO). Briefly, cells were washed with PBS and incubated in pure DMSO for 2 h. After centrifugation at 2000 g for 15 min, capsular PS was isolated from the DMSO fraction and dialyzed against water for 4 days. Then, capsular PS was dried and quantified. The PS was then incubated with 10 mM EDTA overnight at room temperature to remove naturally associated divalent cations. After another dialysis, samples were incubated with different concentrations of $CaCl_2$ (0.2, 2, 6, 10, 15, and 20 mM), and then dialyzed against water to remove the excess unbound cations. Binding of decalcified and Ca^{2+}-treated PSs to polystyrene was then evaluated by enzyme-linked immunosorbent assay (ELISA) using mAb 18B7. Briefly, polystyrene plates were coated with a solution containing 1 μM of the treated PS and the PS was allowed to adhere for 2 h. The plates were then blocked with PBS containing 1% bovine serum albumin. mAb 18B7 (IgG1), was then added to all wells in the plates at a constant concentration of 10 μg/mL. After 1 h, the plates were washed and the binding of mAb was detected using phosphatase-labeled goat antimouse secondary antibodies. The color reactions were developed after the addition of *p*-nitrophenyl phosphate (*p*-NPP) solutions (Sigma, St. Louis, MO), and quantitative determinations were performed by absorbance measurement at 405 nm. All incubations were carried at 37°C for 1 h.

RESULTS

Measurement of bead contact angle with *C. neoformans* capsule by immunofluorescence

The measurement of the elastic properties of the capsule required that we determine the contact angle (α) after adhesion of the polystyrene beads to the capsule of *C. neoformans*. In this context, yeast cells were sequentially incubated with the mAb 18B7 to the capsule and a FITC-secondary antibody was used to visualize primary antibody binding. The cells were placed in the OT system. For attachment to selected yeast cells, the beads were individually pressed against the capsule for 1 min. This procedure was repeated three to five times for each cell examined. Fluorescent images of bead-associated yeast cells were collected (Fig. 2). The angle was determined using the ImageJ software, through the selection of the fluorescent adhesion surface between the labeled capsule and the attached bead. After the analysis of seven beads in three different experiments, an average value of α corresponding to $44 \pm 1^\circ$ was obtained (standard error considered as error bar).

Measurement of *C. neoformans* polysaccharide capsule Young's modulus

Using the measured adhesion angle and the theoretical model described in Materials and Methods, we determined the Young's modulus of the *C. neoformans* capsule. After the attachment of a polystyrene bead to the *Cryptococcus* capsule, the microscope stage was immediately moved with a controlled velocity (V) of 0.071 ± 0.002 μm/s. As a consequence, the selected yeast cell was pulled in the direction of motion, resulting in capsule deformation ($\bar{z} > 0$) and disturbance of the position of equilibrium of the bead ($\Delta\rho > 0$) (Fig. 1 *b*). The measurement of the slope (A) of the curve $\Delta\rho \times t$ allows for determination of the Young's modulus (E) using Eq. 11.

A scheme showing how the $\Delta\rho$ values were obtained is represented in Fig. 3 *a*. The equilibrium position of the bead's center of mass due solely to the optical trap is first measured by image analysis. Coordinate values (x_0, y_0) are used as a reference for zero force. When the stage moves and pulls the *C. neoformans* cell that is attached to the bead, the equilibrium position of the bead changes to new

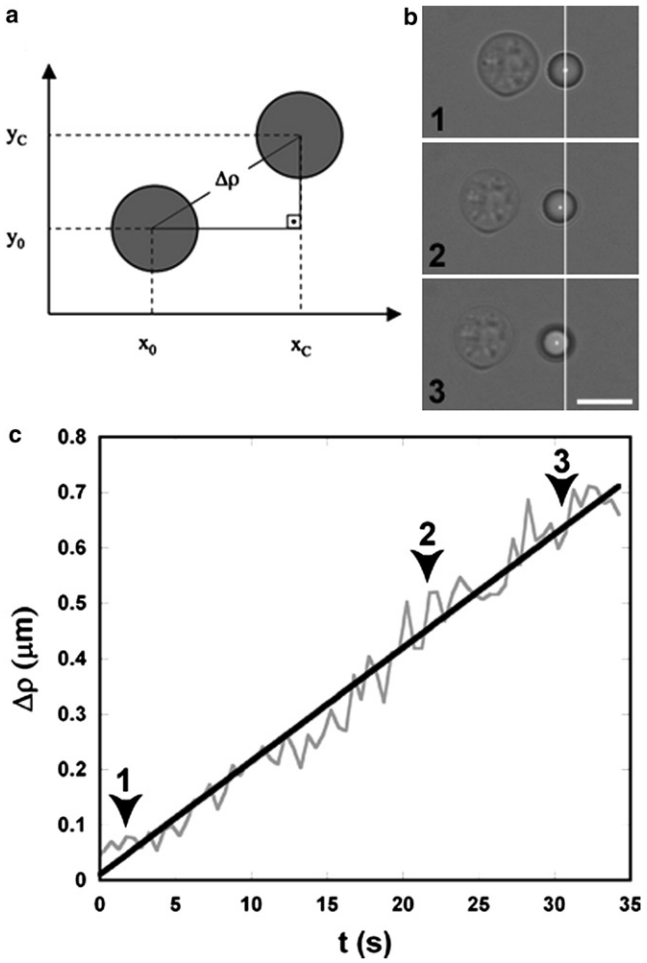

FIGURE 3 Young's modulus determination for the *C. neoformans* capsule. (*a*) Schematic representation of the change in bead position, resulting in displacement from its initial equilibrium position, $\Delta\rho$. (*b*) A sequence of three distinct frames in the same experiment showing the variation in the bead equilibrium position. Scale bar, 5 μm. (*c*) A typical Young's modulus experimental curve under control conditions. For this experiment, the slope of the curve $\Delta\rho \times t$ is $A = 0.021$ μm/s. Using the theoretical model described in the Materials and Methods section, the Young's modulus value determined for this experiment was 77 Pa. Arrowheads 1–3 correspond to the three representative frames shown in Fig. 3 *b*.

coordinate values (x_C, y_C). The variation of the equilibrium position, $\Delta\rho$, is then written as

$$\Delta\rho = \sqrt{(x_c - x_0)^2 + (y_c - y_0)^2}. \quad (12)$$

Fig. 3 *c* and Movie S1 show a typical experimental profile of $\Delta\rho$ variation as a function of time (t), obtained by stretching the capsule in PBS (control condition). The linear dependence of $\Delta\rho$ with time is indicative of elastic solid behavior. Determination of the slope value resulted in $A = 0.021\mu$m/s for this experiment. Using values of $V = 0.071 \pm 0.002$ μm/s, $\alpha = 44 \pm 1°$, $\kappa_\perp = 420 \pm 10\%$ pN/μm, and $a = 1.52 \pm 0.02$ μm, the capsule Young's modulus corresponded to 77 Pa in this individual assay. Thirty-two different measurements were performed under control conditions, giving an $E = 99 \pm 13$ Pa (standard error used as error bar).

Divalent cations influence the elastic properties of the capsule

Divalent cations produce self-aggregation in *C. neoformans* PS fibers (16). Therefore, cation-mediated aggregates and nonaggregated fibers could have different elastic properties. This hypothesis was investigated in experiments using EDTA-pretreated cells that were then incubated in media with different Ca^{2+} concentrations (0–20 mM). The beads did not adhere to the fungal capsule of EDTA-treated cells incubated in ion concentrations ranging from 0 to 2 mM (data not shown), so measurements were not possible for that concentration range. However, at Ca^{2+} concentrations ranging from 6 to 20 mM, the measured values for the Young's modulus increased as a function of ion concentration (Fig. 4 *b*). This effect was accompanied by major morphological changes (Fig. 4 *a*). It is interesting to note that capsule size was reduced when *C. neoformans* was incubated in 20 mM

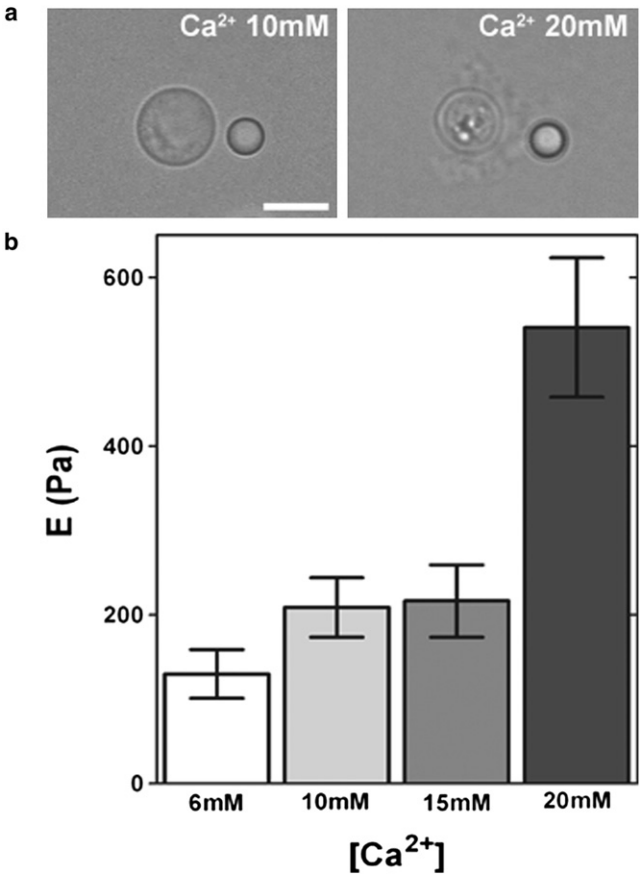

FIGURE 4 Divalent cations influence the elasticity of the *C. neoformans* polysaccharide capsule. (*a*) Representative images of *C. neoformans* after incubation in two different Ca^{2+} concentrations. Scale bar, 5 μm. (*b*) Values of Young's modulus after incubation of *C. neoformans* in different cation Ca^{2+} concentrations. Data are mean ± SE ($n = 20$ cells).

Ca^{2+}, as described previously (16), which led us to hypothesize that smaller capsules were more rigid than larger capsules.

Capsule size and elasticity

Induction of *C. neoformans* capsule occurs during growth in minimal media (14). To establish a relationship between capsule enlargement and elastic properties, we performed experiments to measure the Young's modulus of *C. neoformans* capsule as a function of the fungal growth in vitro (Fig. 5). Capsule sizes of 100 different cells were measured in 24-h intervals over 7 days (Fig. 5 *a*). The elastic modulus of the PS capsule was determined at the same intervals (Fig. 5 *b*). As initially presumed from the result demonstrated in Fig. 4, a clear association between reduced capsule size and reduced elasticity was observed. These results were confirmed by scanning electron microscopy (Fig. 5 *c*). Smaller capsule fibers were visualized clearly at the points where Young's modulus was higher, meaning that capsules with small fibers are less elastic than capsules with bigger ones. Time intervals where the capsular elastic properties were increasing corresponded to yeast with longer capsular fibers (Fig. 5 *d*).

Divalent cations affect binding of mAb 18B7 to *C. neoformans*

Previous studies demonstrated PS self-aggregation in the presence of Ca^{2+} (16). As noted above, our current study revealed an increase in the values of the Young's modulus of PS as a function of Ca^{2+} concentration. We further examined the effect of Ca^{2+} on antibody binding by incubating mAb 18B7 with *C. neoformans* treated with EDTA, which removes preexisting divalent cations. Immunofluorescence studies revealed that the binding of mAb in the presence of Ca^{2+} was more limited to the edge of the capsule compared to control (Fig. 6 *a*). We noted differences in the size of the region that bound to mAb 18B7 (Fig. 6 *b*). The distance from the edge of the cell wall to the beginning of the immunofluorescent region varied in size depending on Ca^{2+} concentration (Fig. 6 *b*).

Divalent cations affect capsular polysaccharide binding to polystyrene

Our observation that OT-manipulated polystyrene beads attach to the capsule of *C. neoformans* implies an affinity between PS and polystyrene. To investigate this property further, we

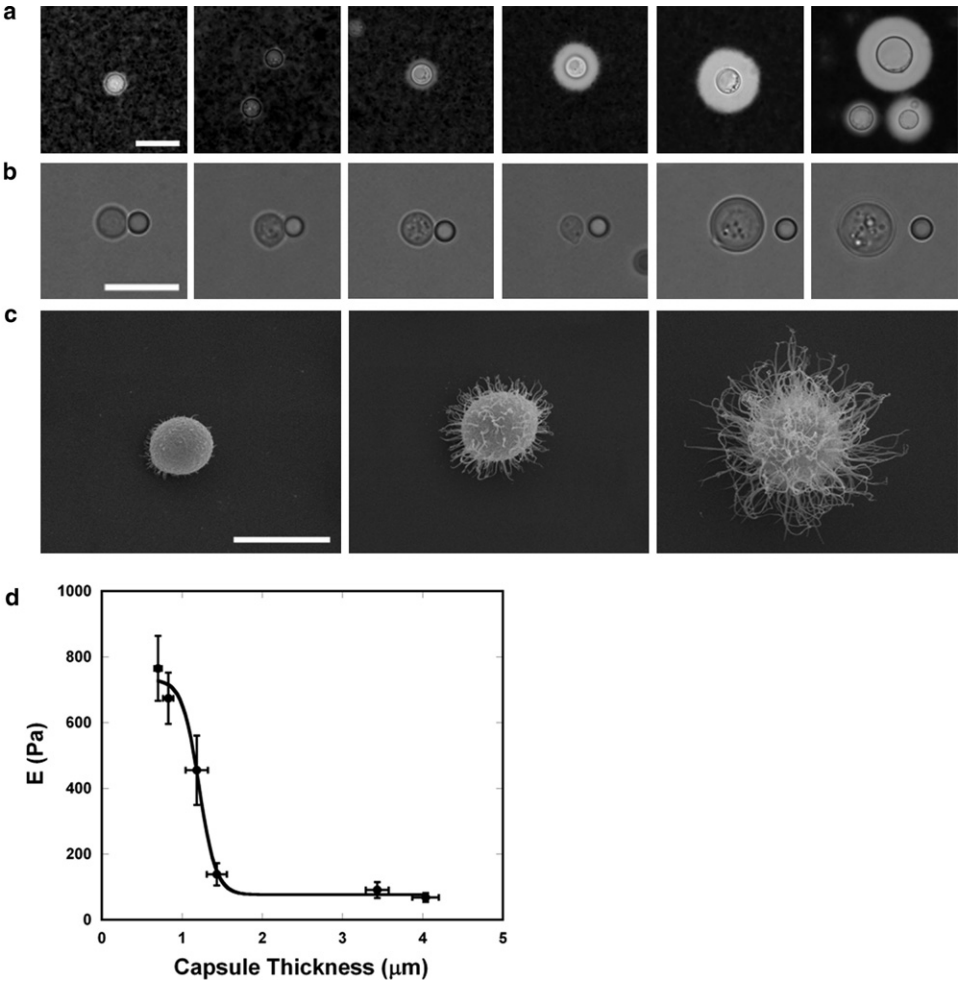

FIGURE 5 Influence of growth time and capsule size on the elastic properties of the *C. neoformans* capsule. (*a*) Representative images of *C. neoformans* cells stained with India ink for each culture interval. Scale bar, 5 μm. (*b*) Representative bright-field images of *C. neoformans* cells used in the Young's modulus experiments. Scale bar, 5 μm. (*c*) Mean ± SE of *C. neoformans* after 1, 3, and 6 days of growth, confirming that the capsule increases as a function of time. Scale bar, 5 μm. (*d*) Plot of the Young's modulus as a function of capsule thickness. Data are mean ± SE.

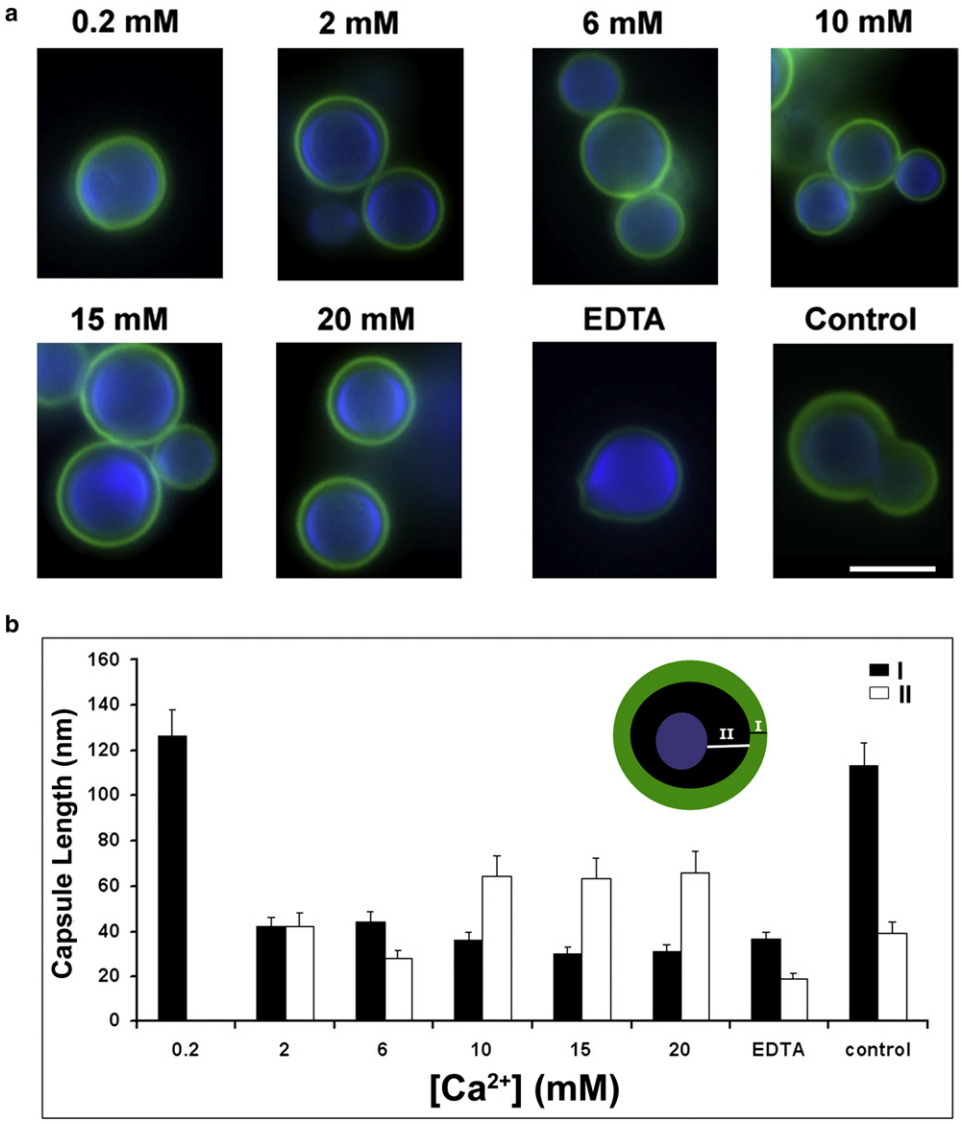

FIGURE 6 Binding of mAb 18B7 to *C. neoformans* cells treated with different concentrations of $CaCl_2$ as revealed by indirect immunofluorescence. (*a*) Fluorescence microscopy revealing mAb 18B7 capsular binding (*green*, FITC) and the fungal cell wall (*blue*, UVITEX). Scale bar, 3 μm. (*b*) Width of the mAb18B7 binding band depended on calcium concentration. The width of 18B7 biding is represented by solid bars. The distance between the cell wall and the edge of mAb binding is represented by open bars. (*Inset*) Illustration of the measured distances. Significant ($p < 0.05$) differences in binding between the samples and control conditions were observed.

developed an ELISA to measure the binding to polystyrene plates of decalcified capsular PS with and without prior incubation in different concentrations of Ca^{2+} (Fig. 7). Decalcification resulted in significantly weaker binding to polystyrene than native PS, which presumably includes cations gathered from growth medium. However, capsular PS treated with Ca^{2+} concentrations >0.2 mM manifested significantly higher binding to polystyrene (Fig. 7), thus providing results in agreement with the observations made with polystyrene beads and cryptococcal capsules.

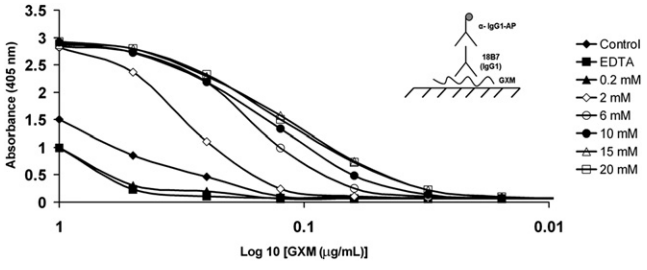

FIGURE 7 Binding of mAb 18B7 to PS-coated polystyrene surfaces as a function of Ca^{2+} and GXM concentrations. The *y* axis represents absorbance at 405 nm.

DISCUSSION

In this study, we investigated the elastic properties of capsular PS by applying force to the capsule of *C. neoformans* and deduced architectural information from the capsule's elastic and mechanical responses. To probe the mechanical properties of the capsule, we developed an OT system where polystyrene beads were pressed onto the external surface of the capsule and then used as handles capable of exerting sufficient force to deform the cryptococcal capsule. By measuring the forces needed for capsular deformation, we determined the capsular Young's modulus in different growth or aggregation

conditions. Although the capsule was known to be a partially deformable structure (27), this study, to our knowledge, provides the first quantitative information on the elastic properties of the capsular network of *C. neoformans*.

The elastic properties of the *C. neoformans* capsule were measured for two conditions that had been known to affect capsular architecture: capsule size and divalent cation concentration. Divalent cations aggregate PS molecules, possibly by forming intra- or intermolecular glucuronic acid residue bridges (16). It has been proposed that this effect contributes to the maintenance of capsular architecture and PS aggregation, and we previously reported that the presence of divalent cations can modify important physical and biological properties of *C. neoformans* PS, including antibody reactivity, electronegativity, and molecular mass (17). Our current results indicate that the elastic properties of the capsule are highly dependent on Ca^{2+} concentration. The observation that capsular elasticity is inversely proportional to Ca^{2+} concentration is consistent with and supports the view that divalent cations create ionic-bond cross-links that stabilize the capsular structure. At higher divalent cation concentrations, all binding sites would be occupied, and this could translate to the formation of a lattice network of cross-linked fibers that would significantly increase the capsule Young's modulus. The location of binding of mAb 18B7 to the capsule was affected by Ca^{2+} concentration, a finding that could reflect differences in capsular permeability to immunoglobulin penetration as a function of PS cross-linking by divalent cations.

The capsular elastic properties varied depending on the capsule size, confirming the highly dynamic nature of this major cryptococcal structure. Variation in capsule thickness, on the other hand, is known to influence fungal pathogenesis in animal models (12). In our model, we found a relationship between capsule size and elasticity, such that larger capsules were more easily deformable by the application of force. This observation may have a correlation with the differential accessibility of the epitope to antibodies that occurs under the different growth conditions used in our experiments (28), and also with the well-known differences observed in the pattern of antibody binding to *C. neoformans* cells (29). The finding that larger capsules are more deformable is consistent with the observation that there is lower density of PS in the outer sections of the capsule (27).

Studies of capsular architecture are stymied by the frailty of these structures. Capsules are highly hydrated structures that are easily disrupted by drying and fixing techniques required for electron microscopy (30). Here, we demonstrate the usefulness of a new approach that could have great applicability for studying capsular properties. The use of polystyrene beads and OT is nondestructive and can be applied to live cells. The Young's modulus values obtained in our study could provide a quantitative parameter for evaluating capsule architecture under different conditions. For example, the conclusion that certain antibodies reduce capsular permeability by cross-linking PS (27,31) can be directly tested by measuring the Young's modulus of cells coated with different types of capsule-binding antibodies. Since modulation of capsular structure by *C. neoformans* has been implicated in such important pathogenic events as extrapulmonary dissemination (32) and fungal crossing of the blood-brain barrier (33), this method could shed light on the relation of capsular mechanical properties and virulence.

An intriguing observation in this study was the relatively stable attachment of inert beads to the capsular network, suggesting that components of the cryptococcal capsule could function as nonspecific adhesive structures. This interaction, which likely involves van der Waals forces, could have a parallel with other adhesive processes involving *C. neoformans*, including biofilm formation and transient binding to host cells. We confirmed this interaction by measuring the binding (ELISA) of isolated PS to polystyrene plates as a function of Ca^{2+} concentration. The finding that binding of GXM to polystyrene increases with Ca^{2+} suggests that divalent cations mediate aggregation by inter- or intramolecular bridges that expose PS domains with affinity to polystyrene. Such nonspecific adhesive properties may be important for holding the capsule together and could precede the formation of more stable interactions, such as those involving GXM and host receptors in phagocytes and epithelial cells (34,35). The OT method could be adapted to investigate this property by evaluating the attachment efficiency of beads with different surface properties.

Recent studies by our group and others have demonstrated that the physical properties of the cryptococcal capsule correlate with its biological functions (16,17). The description of an experimental model in which the capsular flexibility can be precisely determined could be of great relevance to study the affinity of the capsule by biologically active and inert substrates, including a large panel of mAbs raised against capsular components of *C. neoformans* (36). It is important to note that these antibodies have differences in their epitope specificity and ability to modify cryptococcal infections (36). Therefore, in combination with anti-GXM antibodies, measurements of elastic properties of the cryptococcal capsule could be especially relevant in the context of affinity and specificity of capsular components for different surfaces, including host tissues.

SUPPORTING MATERIAL

Additional text, equations, figures, and a movie legend are available at http://www.biophysj.org/biophysj/supplemental/S0006-3495(09)00910-2.

We thank Vivaldo Moura (Neto Universidade Federal do Rio de Janeiro, Rio de Janeiro, Brazil) and Joshua Nosanchuk (Albert Einstein College of Medicine, The Bronx, New York) for discussions and assistance with many aspects of this work.

This work was supported by National Institutes of Health awards AI033774, 5R01HL059842, and 2R37AI033142, and by the Programa de Núcleos de Excelência (MCT/PRONEX), the Brazilian agencies Conselho Nacional de Desenvolvimento Científico e Tecnológico (CNPq), Coordenação de

Aperfeiçoamento de Pessoal de Nível Superior (CAPES), Instituto do Milênio de Nanociências, Instituto do Milênio de Avanço Global e Integrado da Matemática Brasileira, Fundação de Amparo à Pesquisa do Rio de Janeiro (FAPERJ), and Fundação Universitária José Bonifácio (FUJB).

REFERENCES

1. Doering, T. L. 2000. How does *Cryptococcus* get its coat? *Trends Microbiol.* 8:547–553.
2. Casadevall, A., and J. R. Perfect. 1998. *Cryptococcus neoformans*. ASM Press.
3. McFadden, D., O. Zaragoza, and A. Casadevall. 2006. The capsular dynamics of *Cryptococcus neoformans*. *Trends Microbiol.* 14:497–505.
4. McFadden, D. C., M. De Jesus, and A. Casadevall. 2006. The physical properties of the capsular polysaccharides from *Cryptococcus neoformans* suggest features for capsule construction. *J. Biol. Chem.* 281:1868–1875.
5. Cherniak, R., H. Valafar, L. C. Morris, and F. Valafar. 1998. *Cryptococcus neoformans* chemotyping by quantitative analysis of 1H nuclear magnetic resonance spectra of glucuronoxylomannans with a computer-simulated artificial neural network. *Clin. Diagn. Lab. Immunol.* 5:146–159.
6. Zaragoza, O., A. Telzak, R. A. Bryan, E. Dadachova, and A. Casadevall. 2006. The polysaccharide capsule of the pathogenic fungus *Cryptococcus neoformans* enlarges by distal growth and is rearranged during budding. *Mol. Microbiol.* 59:67–83.
7. Kozel, T. R., and E. C. Gotschlich. 1982. The capsule of cryptococcus neoformans passively inhibits phagocytosis of the yeast by macrophages. *J. Immunol.* 129:1675–1680.
8. Kozel, T. R., G. S. Pfrommer, A. S. Guerlain, B. A. Highison, and G. J. Highison. 1988. Role of the capsule in phagocytosis of *Cryptococcus neoformans*. *Rev. Infect. Dis.* 10 (Suppl 2):S436–S439.
9. Zaragoza, O., C. J. Chrisman, M. V. Castelli, S. Frases, M. Cuenca-Estrella, et al. 2008. Capsule enlargement in *Cryptococcus neoformans* confers resistance to oxidative stress suggesting a mechanism for intracellular survival. *Cell. Microbiol.* 10:2043–2057.
10. Zaragoza, O., B. C. Fries, and A. Casadevall. 2003. Induction of capsule growth in *Cryptococcus neoformans* by mammalian serum and CO(2). *Infect. Immun.* 71:6155–6164.
11. Zaragoza, O., and A. Casadevall. 2004. Experimental modulation of capsule size in *Cryptococcus neoformans*. *Biol. Proced. Online.* 6:10–15.
12. Rivera, J., M. Feldmesser, M. Cammer, and A. Casadevall. 1998. Organ-dependent variation of capsule thickness in *Cryptococcus neoformans* during experimental murine infection. *Infect. Immun.* 66:5027–5030.
13. Yoneda, A., and T. L. Doering. 2008. Regulation of *Cryptococcus neoformans* capsule size is mediated at the polymer level. *Eukaryot. Cell.* 7:546–549.
14. Frases, S., B. Pontes, L. Nimrichter, N. B. Viana, M. L. Rodrigues, et al. 2009. Capsule of *Cryptococcus neoformans* grows by enlargement of polysaccharide molecules. *Proc. Natl. Acad. Sci. USA.* 106:1228–1233.
15. Reese, A. J., and T. L. Doering. 2003. Cell wall alpha-1,3-glucan is required to anchor the *Cryptococcus neoformans* capsule. *Mol. Microbiol.* 50:1401–1409.
16. Nimrichter, L., S. Frases, L. P. Cinelli, N. B. Viana, A. Nakouzi, et al. 2007. Self-aggregation of *Cryptococcus neoformans* capsular glucuronoxylomannan is dependent on divalent cations. *Eukaryot. Cell.* 6:1400–1410.
17. Frases, S., L. Nimrichter, N. B. Viana, A. Nakouzi, and A. Casadevall. 2008. *Cryptococcus neoformans* capsular polysaccharide and exopolysaccharide fractions manifest physical, chemical, and antigenic differences. *Eukaryot. Cell.* 7:319–327.
18. Gaboriaud, F., S. Bailet, E. Dague, and F. Jorand. 2005. Surface structure and nanomechanical properties of *Shewanella putrefaciens* bacteria at two pH values (4 and 10) determined by atomic force microscopy. *J. Bacteriol.* 187:3864–3868.
19. Mendelson, N. H., J. E. Sarlls, C. W. Wolgemuth, and R. E. Goldstein. 2000. Chiral self-propulsion of growing bacterial macrofibers on a solid surface. *Phys. Rev. Lett.* 84:1627–1630.
20. Vadillo-Rodriguez, V., T. J. Beveridge, and J. R. Dutcher. 2008. Surface viscoelasticity of individual gram-negative bacterial cells measured using atomic force microscopy. *J. Bacteriol.* 190:4225–4232.
21. Khatri, B. S., M. Kawakami, K. Byrne, D. A. Smith, and T. C. McLeish. 2007. Entropy and barrier-controlled fluctuations determine conformational viscoelasticity of single biomolecules. *Biophys. J.* 92:1825–1835.
22. Viana, N. B., A. Mazolli, P. A. M. Neto, H. M. Nussenzveig, M. S. Rocha, et al. 2006. Absolute calibration of optical tweezers. *Appl. Phys. Lett.* 88:131110.
23. Viana, N. B., M. S. Rocha, O. N. Mesquita, A. Mazolli, P. A. Maia Neto, et al. 2007. Towards absolute calibration of optical tweezers. *Phys. Rev.* 75:021914.
24. Neuman, K. C., and S. M. Block. 2004. Optical trapping. *Rev. Sci. Instrum.* 75:2787–2809.
25. Casadevall, A., W. Cleare, M. Feldmesser, A. Glatman-Freedman, D. L. Goldman, et al. 1998. Characterization of a murine monoclonal antibody to *Cryptococcus neoformans* polysaccharide that is a candidate for human therapeutic studies. *Antimicrob. Agents Chemother.* 42:1437–1446.
26. Laurent, V. M., S. Henon, E. Planus, R. Fodil, M. Balland, et al. 2002. Assessment of mechanical properties of adherent living cells by bead micromanipulation: comparison of magnetic twisting cytometry vs optical tweezers. *J. Biomech. Eng. Trans. ASME.* 124:408–421.
27. Gates, M. A., P. Thorkildson, and T. R. Kozel. 2004. Molecular architecture of the *Cryptococcus neoformans* capsule. *Mol. Microbiol.* 52:13–24.
28. Oscarson, S., M. Alpe, P. Svahnberg, A. Nakouzi, and A. Casadevall. 2005. Synthesis and immunological studies of glycoconjugates of *Cryptococcus neoformans* capsular glucuronoxylomannan oligosaccharide structures. *Vaccine.* 23:3961–3972.
29. Nakouzi, A., and A. Casadevall. 2003. The function of conserved amino acids in or near the complementarity determining regions for related antibodies to *Cryptococcus neoformans* glucuronoxylomannan. *Mol. Immunol.* 40:351–361.
30. Cleare, W., and A. Casadevall. 1999. Scanning electron microscopy of encapsulated and non-encapsulated *Cryptococcus neoformans* and the effect of glucose on capsular polysaccharide release. *Med. Mycol.* 37:235–243.
31. Zaragoza, O., and A. Casadevall. 2006. Monoclonal antibodies can affect complement deposition on the capsule of the pathogenic fungus *Cryptococcus neoformans* by both classical pathway activation and steric hindrance. *Cell. Microbiol.* 8:1862–1876.
32. Luberto, C., B. Martinez-Marino, D. Taraskiewicz, B. Bolanos, P. Chitano, et al. 2003. Identification of App1 as a regulator of phagocytosis and virulence of *Cryptococcus neoformans*. *J. Clin. Invest.* 112:1080–1094.
33. Charlier, C., F. Chretien, M. Baudrimont, E. Mordelet, O. Lortholary, et al. 2005. Capsule structure changes associated with *Cryptococcus neoformans* crossing of the blood-brain barrier. *Am. J. Pathol.* 166:421–432.
34. Barbosa, F. M., F. L. Fonseca, R. T. Figueiredo, M. T. Bozza, A. Casadevall, et al. 2007. Binding of glucuronoxylomannan to the CD14 receptor in human A549 alveolar cells induces interleukin-8 production. *Clin. Vaccine Immunol.* 14:94–98.
35. Levitz, S. M. 2004. Interactions of toll-like receptors with fungi. *Microbes Infect.* 6:1351–1355.
36. Nakouzi, A., P. Valadon, J. Nosanchuk, N. Green, and A. Casadevall. 2001. Molecular basis for immunoglobulin M specificity to epitopes in *Cryptococcus neoformans* polysaccharide that elicit protective and nonprotective antibodies. *Infect. Immun.* 69:3398–3409.